Taylor & Francis
Taylor & Francis Group

Hydrological Sciences Journal

ISSN: (Print) (Online) Journal homepage: https://www.tandfonline.com/loi/thsj20

Differential response to rainfall of soil moisture infiltration in permafrost and seasonally frozen ground in Kangqiong small basin on the Qinghai-Tibet Plateau

Wei Cao, Yu Sheng, Jichun Wu & Erxing Peng

HYDROLOGICAL SCIENCES JOURNAL
2021, VOL. 66, NO. 3, 525–543
https://doi.org/10.1080/02626667.2021.1883619

Differential response to rainfall of soil moisture infiltration in permafrost and seasonally frozen ground in Kangqiong small basin on the Qinghai-Tibet Plateau

Wei Cao, Yu Sheng, Jichun Wu and Erxing Peng

State Key Laboratory of Frozen Soil Engineering, Northwest Institute of Eco-Environment and Resources, Chinese Academy of Sciences, Lanzhou, China

ABSTRACT
This study investigated the differential response to rainfall of soil moisture infiltration in the permafrost area of the downhill slope and in the seasonally frozen ground area of the uphill slope in Kangqiong small basin on the Qinghai-Tibet Plateau. The results show that: (1) influenced by the barrier of the permafrost layer, the suprapermafrost water level in the permafrost area rises significantly, while in the seasonally frozen ground area, the soil moisture infiltration is dominated by lateral flow and downward infiltration. (2) With the thawing of soil, the soil water content in the permafrost area gradually increases to reach a saturated state. Influenced by terrain, soil texture, evapotranspiration and infiltration capacity, the variation in the topsoil moisture content is large in the seasonally frozen ground area. (3) The presence of regional talik groundwater leads to a slight increase in the water level on the uphill slope. In addition to rainfall infiltration, the change in water level on the downhill slope is also affected by talik groundwater, which causes the rapid rise of water level on the down slope.

ARTICLE HISTORY
Received 10 September 2019
Accepted 18 November 2020

EDITOR
A. Fiori

ASSOCIATE EDITOR
O. Makarieva

KEYWORDS
differential response; soil moisture infiltration; permafrost; seasonally frozen ground; Qinghai-Tibet Plateau

1 Introduction

Permafrost is extremely sensitive to temperature change. As permafrost changes due to climate warming and human activities, this will have an important impact on the ecological and hydrological environment in cold regions. This is mainly because permafrost is the major controlling factor in the geological environment of cold regions (Zhang *et al.* 2015, Bibi *et al.* 2018). Currently, with the continuous intensification of climate warming and human activities, the permafrost has undergone large-scale degradation, as evidenced by a deepening active layer, reduction in permafrost thickness, rising ground temperatures, expansion of taliks, and disappearance of patchy permafrost. Because permafrost is an important component in cold regions, this degradation is resulting in significant changes to the vertical profile thickness and horizontal distribution boundary of permafrost, and, moreover, has brought about marked changes in the structural composition and distribution pattern of the biosphere in cold regions (Jorgenson *et al.* 2010, Zhang 2012, Chang *et al.* 2015, Jones *et al.* 2016). In particular, permafrost degradation under the influence of global climate change has changed the migration process of surface soil moisture and has profoundly affected the regional water cycle and water balance (Woo *et al.* 2008, Jepsen *et al.* 2013, Oliva *et al.* 2018). Therefore, studying the infiltration process of surface soil moisture in permafrost regions will deepen our understanding of permafrost change and its hydrological effects against a background of global climate change. It will also play a positive role in understanding how water resources are being changed by permafrost degradation.

Soil moisture movement in permafrost regions varies under the influence of the freeze–thaw process. Studies on this theme have attracted the attention of scholars around the world. Recent research has focussed on analysing the soil moisture characteristics of the active layer in permafrost regions and in seasonally frozen ground regions. Based on laboratory tests and field observations, these studies emphasize the change in soil moisture content and its coupling relationship with soil temperature during freeze–thaw periods (Hinkel *et al.* 2001, Subin *et al.* 2013; Schuh *et al.* 2017, Li *et al.* 2012, Zhao *et al.* 2019). In addition, the response process of soil moisture movement under different underlying surface conditions in permafrost regions has been studied in depth. In particular, the underlying surface conditions involve factors such as land-cover type, vegetation coverage and snow cover in permafrost regions. The effects of these natural environmental factors on the soil moisture transport process under the influence of the freeze–thaw process are systematically studied, revealing the movement processes of soil moisture in permafrost regions and in seasonally frozen ground regions under different freeze–thaw stages.

Meanwhile, scientists also study the response of soil moisture in permafrost regions and in seasonally frozen ground regions to different influencing factors, from different perspectives (Hu *et al.* 2009, Wang *et al.* 2009, Guan *et al.* 2010a, 2010b, Yang *et al.* 2011). However, soil moisture is the link between surface water and groundwater. Precipitation is the main driving force for soil moisture movement in permafrost regions. At the same time, the soil moisture in permafrost

CONTACT Yu Sheng sheng@lzb.ac.cn State Key Laboratory of Frozen Soil Engineering, Northwest Institute of Eco-Environment and Resources, Chinese Academy of Sciences, Lanzhou 730000, China

regions will be further transferred into superpermafrost water through the form of interflow. However, this hydrological process is extremely complex (Jafarov *et al.* 2018, Lamontagne-Halle *et al.* 2018). Consequently, there are relatively few studies on the transport process and infiltration process of permafrost soil moisture from the perspective of the source and sink of soil moisture.

Qinghai-Tibet Plateau, especially the Source Area of the Yellow River (SAYR) in the northeast, is the birthplace of major rivers in China and Asia. In recent years, the climate there has become significantly warmer, leading to the accelerating degradation of the permafrost on the plateau. Under the influence of permafrost degradation, the water supply, runoff and discharge processes of the SAYR have changed significantly. Therefore, there is an urgent need to understand the hydrological impact of permafrost change (Wu and Zhang 2008, Cheng and Jin 2013, Wang *et al.* 2017, Chang *et al.* 2018).

To this end, this study takes the permafrost area and the seasonally frozen ground area of Kangqiong small basin in the SAYR as an example. The processes of soil moisture transport in the permafrost area and seasonally frozen ground area are studied from a source–sink perspective. We mainly consider the variation of rainfall and superpermafrost water in the study area. We use field observations and numerical simulation synthetically to analyse the differential response mechanism of soil moisture infiltration to rainfall in the typical permafrost area and seasonally frozen ground area in the SAYR. This research can provide the scientific basis for a deep understanding of the effect of permafrost degradation on water resources.

2 Materials and methods

2.1 Study area

The SAYR (33°56′–35°31′N, 95°55′–98°41′E; 4193–5238 m a.s.l.) is located in the east-central part of Qinghai-Tibet Plateau. The name SAYR generally refers to the catchment area of the headwater of the upper reach of Doushi Gorge, in particular to the catchment centre of two lakes (E'ling and Zaling lakes). The total area is about 2.98×10^4 km^2. The geomorphic types in the source area are complex and diverse, covering glacial-erosion valleys, plateau mountains, steep slopes, gentle slopes, river-facies beaches, beach plains, and deep hills. In addition to E'ling Lake and Zaling Lake, there are many plateau lakes in this region, such as Longre Cuo, Chamu Cuo, Galala Cuo, and Xingxinghai. In addition, surface water in this region includes the rivers Duo Qu, Re Qu, Lena Qu and Beimin Qu, which are the primary tributaries of the Yellow River. The SAYR is situated in the plateau continental-climate zone, which is influenced by a monsoon climate. The annual precipitation and evaporation in this region are 300–400 mm and 300–500 mm, respectively, and the mean annual temperature is less than −3.5°C. This region is covered by alpine marsh meadow, alpine meadow, plateau grassland, and desert as the main vegetation types.

The lower limit of permafrost in the SAYR is generally 4350–4370 m. More than 80% of the region is covered by permafrost. The mean annual ground temperature (MAGT) below 15 m depth is between −0.2°C and 2°C, and the active layer thickness (ALT) is between 0.6 m and 3 m. In recent years, permafrost has been gradually degraded due to climate warming and human activities. As a result of our field investigation, we selected Kangqiong small basin in the SAYR as the study region, mainly because this area is simultaneously covered by permafrost and seasonally frozen ground. The downhill slope of Kangqiong small basin (4302 m a.s.l.) is mainly covered by discontinuous permafrost. The landform is characterized by a valley basin, and the surface vegetation is mainly *Carex* grassland. The permafrost thickness is 30–50 m and the seasonally thawed depth is 2.8 m. The MAGT in this downhill area is −0.57°C. According to the relationship between MAGT and the stages of permafrost degradation (Jin *et al.* 2006, Wu *et al.* 2010), this area is in the early to middle stage of permafrost degradation. This means that although the ground temperature is still rising to a certain extent, it is in a relatively stable stage of permafrost. So, the downhill slope of Kangqiong small basin represents a typical permafrost area.

The uphill slope of Kangqiong small basin (4314 m a.s.l.) is mainly covered by seasonally frozen ground. The landform is characterized by a mild slope topography, which is mainly covered by bare desert with sparse vegetation and some secondary weeds. The MAGT in this uphill area is 0.95°C. This means that this area is in the phase of permafrost disappearance. So, the uphill area of Kangqiong small basin represents a typical seasonally frozen ground area.

2.2 Sampling method

For research purposes, we chose a vertical section in Kangqiong small basin (Fig. 1). Two slope positions were chosen in the vertical section, from the uphill to the downhill. Using a drilling rig of hydraulic type 100, we excavated two permafrost boreholes to a depth of 20 m in order to monitor ground-temperature characteristics at different depths in different periods. The bore diameter of the permafrost borehole was approximately 127 mm. To monitor the ground-temperature data, we embedded temperature probes at depths of every 0.5 m or 1.0 m in the permafrost borehole and placed a steel pipe in the permafrost borehole to protect these probes after the embedding was completed. The temperature probes were thermistor probes, produced by the State Key Laboratory of Frozen Soil Engineering, Chinese Academy of Sciences. This type of probe has good stability of performance, mature technology capacity, and long service time. Its measuring precision is better than 0.05°C and its range of operating temperature is between −30 and +30°C. The resolution of the probe is 0.01–0.005°C (negative temperature) and 0.01–0.03°C (positive temperature). We periodically measured the resistance values of each temperature probe using a high-precision multimeter (Fluke 287/289). The resistance values could be converted to temperature values using the calibration parameters of each probe.

High-density electrical method (ERT) exploration was carried out in the vertical section from uphill to downhill in Kangqiong small basin. Two survey lines were laid to make a thorough investigation of the general situation of the permafrost and hydrogeology in the region. The instrument for ERT data collection was the 8-channel ERT instrument

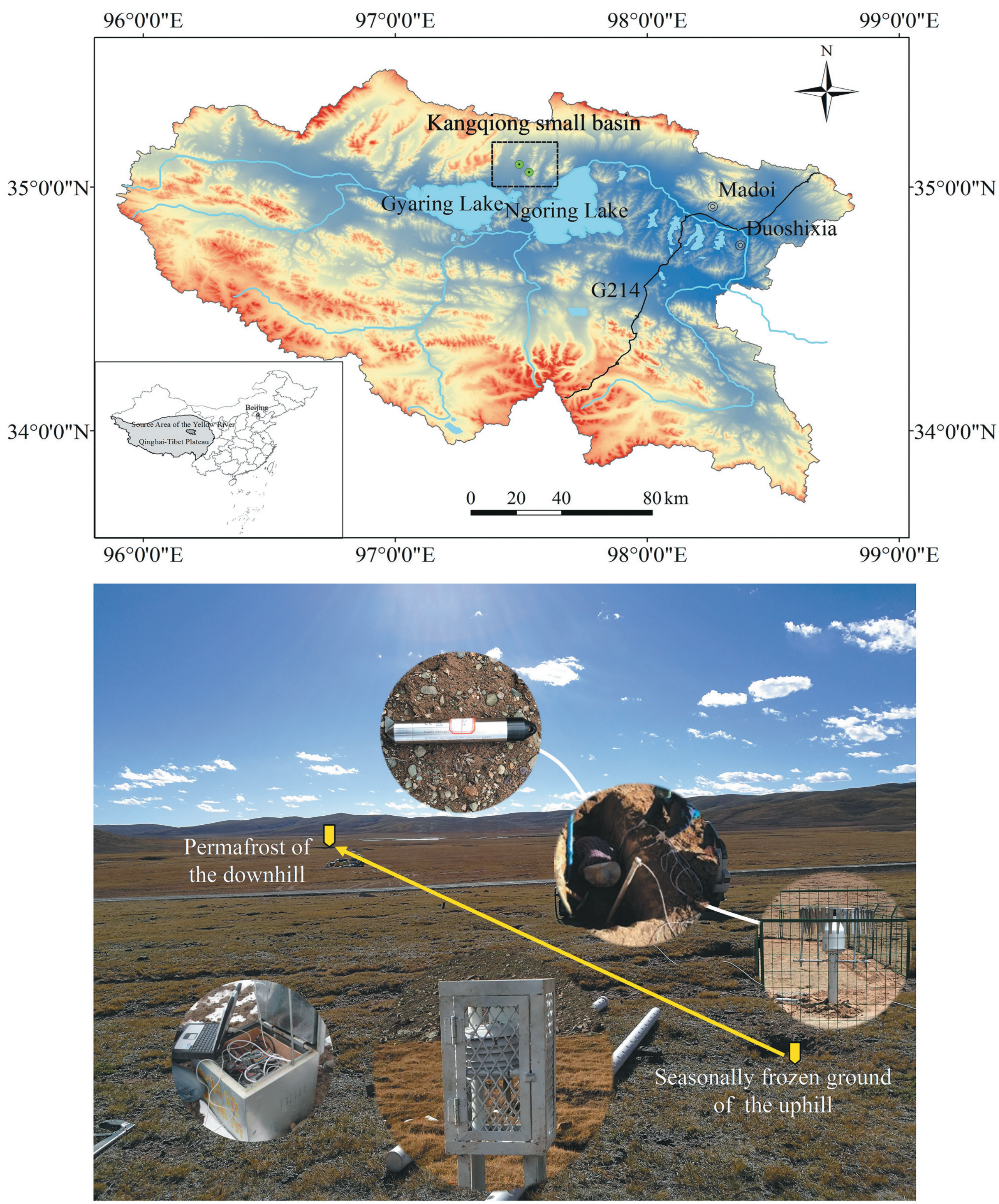

Figure 1. Field monitoring site of the study area.

(SUPERSTING R8) produced by the American AGI Corporation. It can measure up to eight sets of data at the same time. Using the Wenner-Schlumberger device, we placed electrodes at 5 m spacing. The measuring line, which was 200–400 m long, could monitor the resistivity value from 30 to 80 m below the surface.

At the same time, we installed a series of monitoring instruments inside the slope positions. These instruments included soil temperature probes and soil moisture probes produced by the Onset Corporation of America. In the permafrost area, these probes were embedded at depths of 20, 50, 80, 120, 160, 200 and 250 cm in the downhill slope position; and in the seasonally frozen ground area, the probes were embedded at depths of 20, 50, 80, 120, 160 and 200 cm in the upper slope position. The measuring precision of the soil temperature probe (S-TMB-M006) is less than 0.2°C. The operating temperature of the soil temperature probe is from −40°C to +70°C and the observation accuracy of the soil moisture probe (S-SMC-M005) is 3%. The operating temperature of the soil moisture probe is from 0°C to 50°C. For data acquisition we employed the CR3000 instrument, produced by the Campbell Corporation of America, to acquire soil temperature and soil moisture data once every 4 h.

In addition, we established the observed suprapermafrost water-level wells near the permafrost boreholes. The suprapermafrost water-level pipe is made of aluminum-plastic polypropylene random (PPR) piping, chosen mainly because it is made of sturdy material. It is frost-resistant and wear-resistant in high altitudes and alpine regions. The inner diameter of this pipe is 45 mm and the diameter of the hole drilled in the tube wall is 5–10 mm. The suprapermafrost water-level pipes were embedded in the two observed wells. To prevent the fine sand and clay from falling into the suprapermafrost water-level pipe, a plastic filter screen was wrapped around the outside of the pipe. We used a HOBO U20 Water Level Logger to monitor changes in the suprapermafrost water level. The product model is U20-001-04. Its measuring precision is less than 0.3 cm and the range of operating temperature is from −20 to +50°C. The suprapermafrost water-level logger was fixed together with nylon rope and wire rope. Two suprapermafrost water-level loggers were placed at the lower part of the suprapermafrost water-level pipe, one in the uphill slope position and one in the downhill slope position. Their monitoring frequency was also once every 4 h. We chose to monitor data during the thawing period from May to October 2017.

We used a HOBO U23-001 (HOBO Pro v2) temperature-humidity recorder to observe the atmospheric temperature. To avoid being influenced by the outside environment, the recorder, which was placed in a radiation protection hood, was installed in a steel louver, and the device was buried at the observation site with the top about 1 m above the surface. The measuring precision of the temperature-humidity recorder is ±0.2°C, the operating temperature is from −40°C to +70°C, and the resolution ratio is 0.02°C. We employed the optical base and connector set of HOBO BASE-U-4 to acquire the atmospheric temperature and humidity data once every 30 min.

Precipitation was observed using a T-200B automatic rain-snow gauge, manufactured by the Norwegian Geonor Corporation. Because the gauge uses a vibrating wire-weighing sensor, it was fixed on the concrete-casting base to maintain the stability of the sensor. It was simultaneously equipped with a metal windshield around the gauge. To maintain the accuracy of data acquisition, we added antifreeze to thaw the solid-state precipitation and added engine oil to prevent evaporation loss in the automatic rain-snow gauge reservoir. The total capacity of the reservoir was 600 mm. The measuring precision of the temperature-humidity recorder is 0.1% FS, the operating temperature is from −40°C to +60°C, and the sensitivity is 0.05 mm.

2.3 Research methods

Without considering the lateral flow of groundwater, the vertical infiltration process of precipitation in permafrost and seasonally frozen ground area is mainly simulated by the freeze–thaw module of HYDRUS-1D software (Hansson *et al.* 2004, Zhao *et al.* 2016, Dagois *et al.* 2017).

2.3.1 Equation of soil moisture movement and heat flow

This module improves the Richards equation by coupling the soil hydrothermal process. So it can simulate the soil moisture movement in the freeze–thaw period. The equation can be written as follows:

$$\frac{\partial\theta_u(h)}{\partial t}+\frac{\rho_i}{\rho_w}\frac{\partial\theta_i(T)}{\partial t} = \frac{\partial}{\partial z}\left[K_{Lh}(h)\frac{\partial h}{\partial z}+K_{Lh}(h)+K_{Lh}(h)\frac{\partial T}{\partial z} +K_{vh}(\theta)\frac{\partial h}{\partial z}+K_{vT}(\theta)\frac{\partial T}{\partial z}\right]-S \tag{1}$$

where θ_u denotes the volumetric unfrozen water content (including volumetric liquid and vapor water content), cm^3/cm^3; θ is the volumetric liquid content, cm^3/cm^3; θ_i represents the volumetric ice content, cm^3/cm^3; t is time, s; z is the spatial coordinate, cm, and upward is positive; ρ_i denotes the ice density, kg/m^3, taking a value of 931 kg/m^3; ρ_w represents the density of liquid water, kg/m^3, taking a value of 1000 kg/m^3; h is the pressure head, cm; T is the temperature, K; S is a sink or source term, s^{-1}, which is normally root extracted.K_{Lh}, K_{Lt}, K_{vh} and K_{vT} are, respectively, liquid hydraulic conductivity under the action of water potential, liquid hydraulic conductivity under the action of temperature, gaseous hydraulic conductivity under the action of water potential and gaseous hydraulic conductivity under the action of temperature.

The heat flow equation in the model is expressed as follows:

$$\frac{\partial C_pT}{\partial t}-L_f\rho_i\frac{\partial\theta_i}{\partial t}+L_0(T)\frac{\partial\theta_v(T)}{\partial t} =\frac{\partial}{\partial z}[\lambda(\theta)\frac{\partial T}{\partial z}]-C_w\frac{\partial q_1T}{\partial z}-C_v\frac{\partial q_vT}{\partial z}-L_0(T)\frac{\partial q_v}{\partial z}-C_wST \tag{2}$$

where$\theta_v$denotes the gaseous water content, cm^3/cm^3.$L_0=L_w\rho_w$, $L_w$is the latent heat of water gasification, where the value is taken as $2.501\times10^6-2369.2T$, J/kg. L_f represents the latent heat of water freezing, where the value is taken as approximately 3.34×10^5, J/kg. $\lambda(\theta)$ is the soil thermal conductivity, $W/(m{\cdot}°C)$. q_1 denotes the liquid water flux, m/s. C_p represents the soil volume heat capacity, J/(m^3·K^{-1}), which is the sum of the heat capacity of each phase (solid phase C_n, liquid phase C_w, vapor phase C_v and ice phase C_i) in the soil.

Equations (1) and (2) are closely coupled. Both equations depend on water content, pressure head and temperature, and are interrelated in the solving process. The finite difference method is used to solve the equations of water and heat dynamics. And the coupling relationship between water and heat flow is considered to solve the model iteratively.

2.3.2 Initial and boundary conditions

The results of linear interpolation to the measured soil moisture can be used as the initial condition of the model at the beginning of simulation period.

Because the water content of the surface soil in the active layer of permafrost varies with time during the thawing period, the upper boundary condition of the model must consider surface water accumulation in this period. In this paper, the maximum stagnation depth of surface water is set at 10 cm. When the rainfall exceeds the maximum stagnation depth, the stagnation depth will not increase, and the excessive seepage water will form surface runoff. In the simulation period, the upper boundary flux values, including rainfall and evaporation, are input daily into the model. The lower boundary is set at 250 cm. Considering that the permafrost table is 280 cm and the corresponding suprapermafrost water level is 280 cm, the free drainage boundary is adopted. The boundary conditions can be expressed as:

$$\begin{cases} K(h)\frac{\partial h}{\partial z} - K(h) = q_0(0,t) - \frac{dh}{dt} & h_a \le h \le h_s \quad z=0, t>0 \\ h = h_a \quad h < h_a & h<h_a \quad z=0, t>0 \\ \left[\frac{\partial h}{\partial z}\right]_{z=250} = 0 & t>0 \end{cases} \quad (3)$$

where$q_0$denotes the net infiltration rate (that is, the difference between rainfall and evaporation), cm/d.$h_a$represents the minimum pressure water head on the surface, which is set as −100 000 cm in this study. h_s is the maximum stagnant depth of surface water, and is taken as 10 cm in the model.

2.3.3 Soil hydraulic parameters

This module describes the soil water characteristic curve $\theta(h)$ and unsaturated hydraulic conductivity $K(h)$ by the van Genuchten-Mualem model:

$$\theta(h) = \begin{cases} \theta_r + \frac{\theta_s - \theta_r}{[1+|\alpha h|^n]^m} & h < 0 \\ \theta_s & h \ge 0 \end{cases} \quad (4)$$

$$K(h) = K_s S_e^l [1 - (1 - S_e^{1/m})^m]^2 \quad (5)$$

$$S_e = \frac{\theta - \theta_r}{\theta_s - \theta_r} m = 1 - \frac{1}{n}, n > 1$$

where θ_s denotes saturated soil water content, cm^3/cm^3. θ_r is the residual water content in soil, cm^3/cm^3. K_s represents the saturated hydraulic conductivity, cm/d. α(cm^{-1}), n are the shape parameter. $l$is the bending parameter.

2.3.4 Verification of results

According to the soil genetic horizon, the soil in the simulation process is divided into seven layers and six layers in the permafrost and the seasonally frozen ground, respectively (0–20 cm, 20–50 cm, 50–80 cm, 80–100 cm, 100–160 cm, 160–200 cm; 200–250 cm). At the same time, it is assumed that the soil properties in each layer are uniform. Based on the measured soil particle composition and bulk density of each layer, the hydraulic parameters of each layer were predicted by using the neural network module in HYDRUS-1D as the initial value.

In this study, the correlation coefficient (R^2) was used to evaluate the simulation results. Figure 2a shows a comparison of the results for soil temperature and soil moisture of seven soil layers (20 cm, 50 cm, 80 cm, 120 cm, 160 cm, 200 cm, 250 cm) simulated by the model and the measured values. The simulation value is essentially consistent with the measured value in the change trend, which shows that the simulation result of the model is good.

3 Results

3.1 Changes in soil temperature of permafrost and seasonally frozen ground

Figure 3 shows the changes of atmospheric temperature and precipitation in the study area from May to October 2017. It can be seen from the figure that the mean temperature in the area during this period was 6.06°C. The highest temperature was 15.1°C, on 21 July 2017, and the lowest was −2.16°C, on 15 May 2017. The cumulative precipitation during this period was 356.2 mm. Due to the rainfall being relatively high during this period, there was abundant water.

Figure 4 shows a contour map of the soil temperature in the permafrost area of the downhill slope and in the seasonally frozen ground of the uphill slope. It can be seen from the figure that the gradient of the zero-degree isotherm in the permafrost area of the downhill is slightly in the stage of thawing. This indicates that it will take a long time for the soil of the active layer to thaw completely at a depth of 250 cm.

Soil temperature contours are slightly dense, indicating that the rate of temperature rise is faster. The time interval of the initial date of soil thawing at different depths is larger, which indicates that the deep soil lags obviously behind the shallow soil. Moreover, the gradient of the zero-degree isotherm in the seasonally frozen ground area of the uphill slope is steep in the stage of thawing, indicating that it will take a shorter time for the soil to thaw completely at a depth of 200 cm. Soil temperature contours are slightly sparse, indicating that the rate of temperature rise is slower. The time interval between the initial dates of soil thawing at different depths is small, which indicates that the deep soil lags slightly behind the shallow soil.

3.2 Permafrost hydrogeological characteristics

Figure 5 shows the ERT inversion results of permafrost and seasonally frozen ground. According to the results of the analysis, a resistivity value greater than 250 Ω·m is considered high in Kangqiong small basin. The sub-regions with resistivity of less than 100 Ω·m are considered to be suprapermafrost water; the sub-regions with resistivity between 100 Ω·m and 250 Ω·m are considered to be talik; and the sub-regions with resistivity greater than 250 Ω·m are considered to be permafrost or bedrock (strongly weathered mudstone). It can be seen from Fig. 5 that the distribution of high resistivity value is discontinuous in the downhill slope. The area with resistivity greater than 250 Ω·m is mainly located within the region 20–60 m below the surface. To monitor ground temperature, there is a permafrost borehole at 20 m depth at about 170 m along the horizontal direction of the ERT exploration line. The

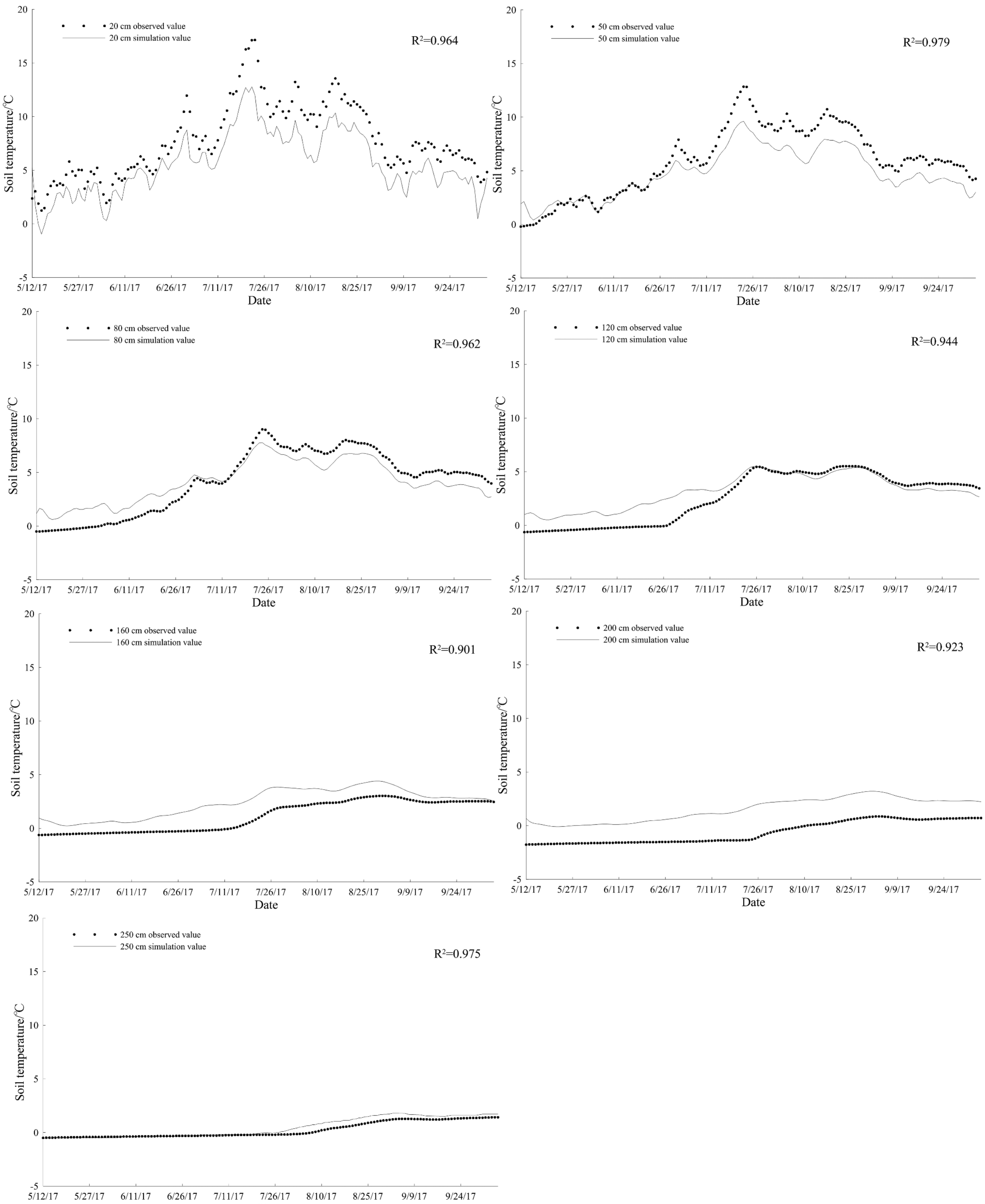

Figure 2a. Comparison of simulation results of soil temperature and moisture at different depths. (a) Soil temperature of permafrost of the downhill slope.

monitoring data of the permafrost borehole show that the MAGT in this zone is −0.57°C, which is inferred to be permafrost. The resistivity value is lower than 100 Ω·m at 0–100 m in the horizontal direction and at 2 m in the vertical direction along the exploration line, and it is inferred that this region is the suprapermafrost water. The resistivity value is between 100 Ω·m and 250 Ω·m at 0–220 m in the horizontal direction along the exploration line, which is inferred to be the talik.

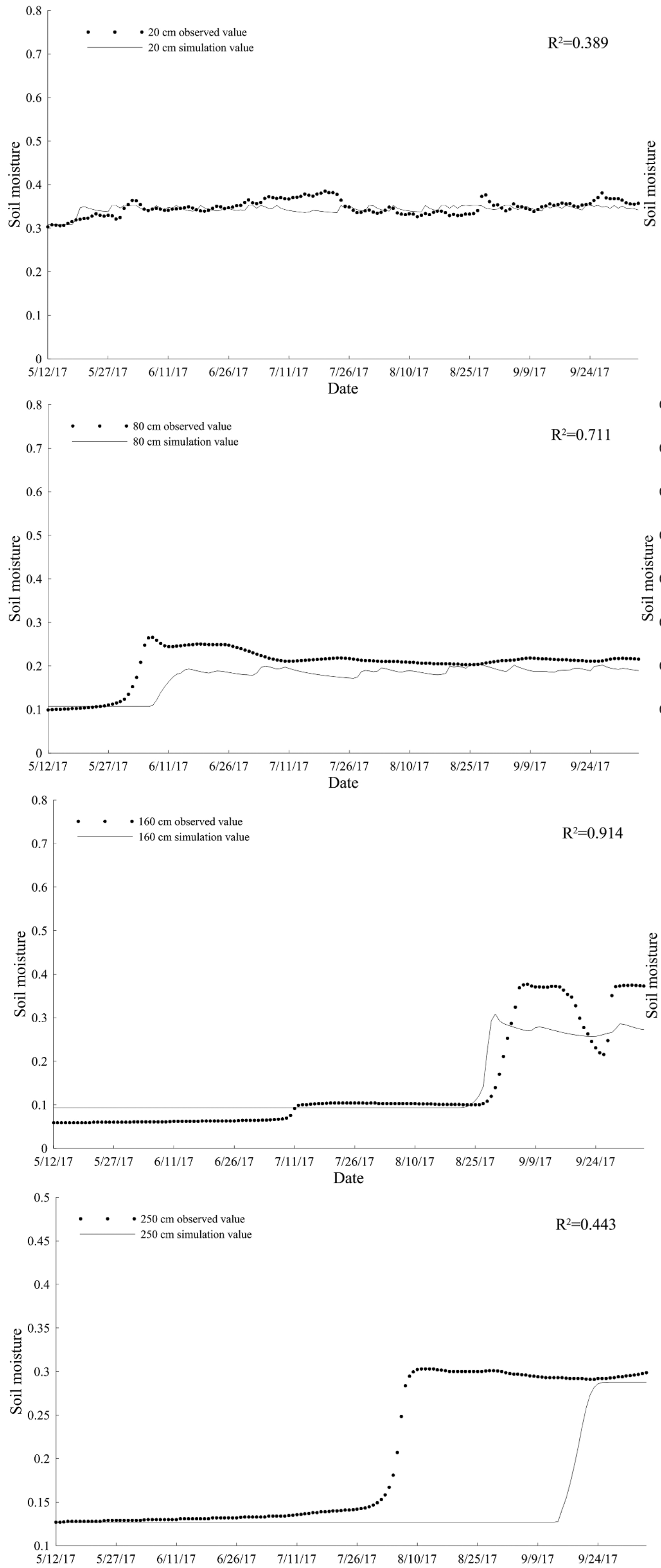

Figure 2b. Comparison of simulation results of soil temperature and moisture at different depths. (b) Soil moisture of permafrost of the downhill slope.

Based on the above analysis, it is inferred that the zone in the downhill slope is in the permafrost area. As can be seen from Fig. 5, the distribution of high resistivity values is discontinuous in the uphill area. The range with resistivity greater than 250 Ω·m is mainly located within the zone 20–60 m below the surface, and the resistivity of this region is in

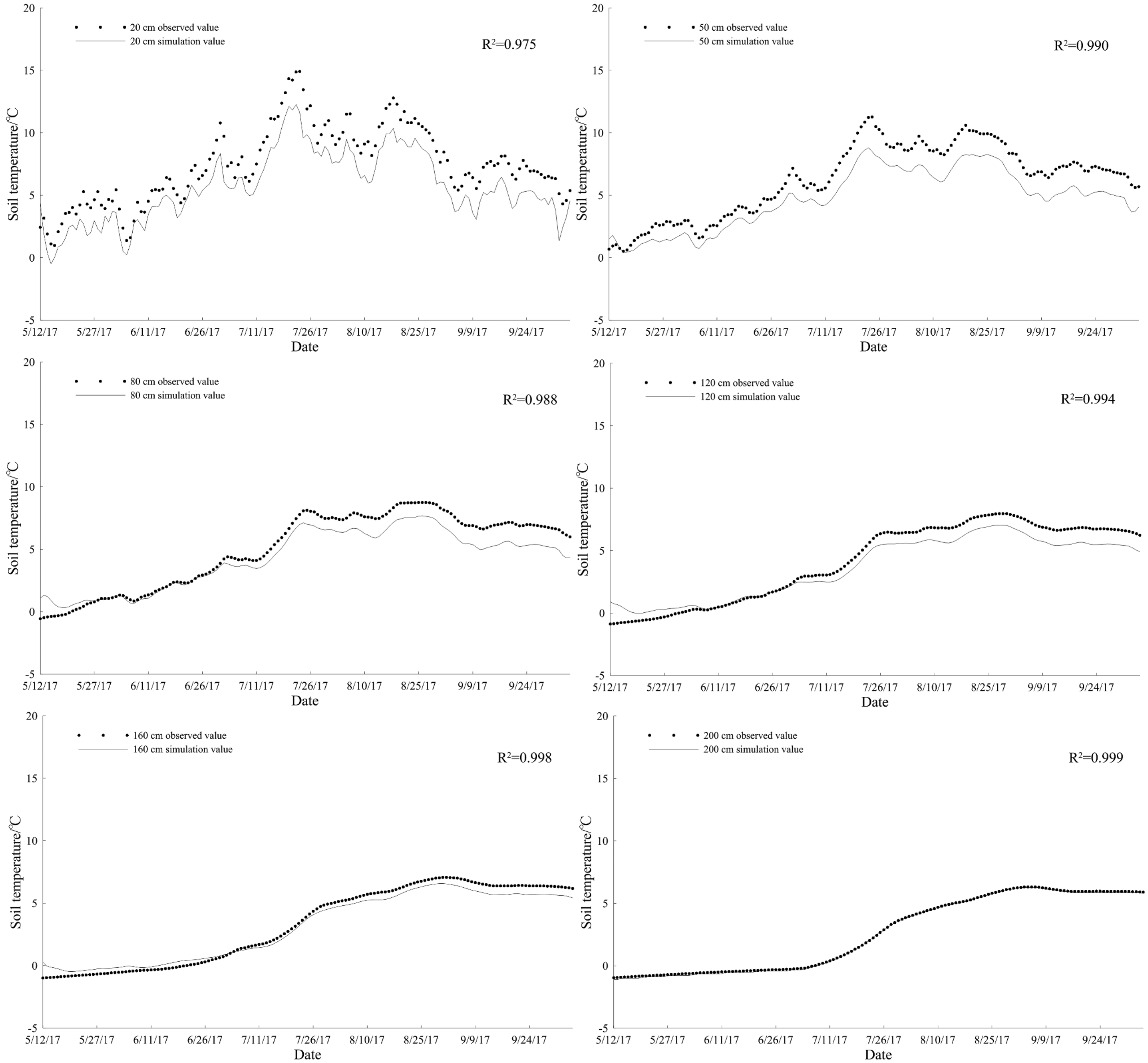

Figure 2c. Comparison of simulation results of soil temperature and moisture at different depths. (c) Soil temperature of seasonally frozen ground of the uphill slope.

the range 400–600 Ω·m. To monitor ground temperature, we excavated a permafrost borehole with a depth of 20 m at about 70 m along the horizontal direction of the ERT exploration line. The monitoring data from the permafrost borehole show that the MAGT in this zone is 0.95°C, which we infer to be strongly weathered mudstone. Among the data, the resistivity value is lower than 100 Ω·m at 0–120 m in the horizontal direction and at 2 m in the vertical direction along the exploration line. It is inferred that this area is the suprapermafrost water. The resistivity value is between 100 Ω·m and 250 Ω·m at 0–280 m in the horizontal direction along the exploration line, which is inferred to be the talik. High resistivity values appear in the range of 0–10 m below the surface in the horizontal direction of 160–180 m and 280–350 m along the exploration line. Based on the above analysis, it is inferred that the area of the uphill slope is in the last stage of permafrost degradation or has already degenerated into seasonally frozen ground.

3.3 Process of soil moisture infiltration in permafrost and seasonally frozen ground under the change of rainfall season

3.3.1 Permafrost

Figure 6 shows the seasonal change in the soil moisture of permafrost and the seasonally frozen ground. It can be seen from the figure that as the soil in each layer begins to thaw in the rapid thawing stage, soil moisture gradually improves in the permafrost area of the downhill slope. Because the surface soil thawed before the bottom soil, the bottom soil was still in a completely frozen state. This led to the water content of the

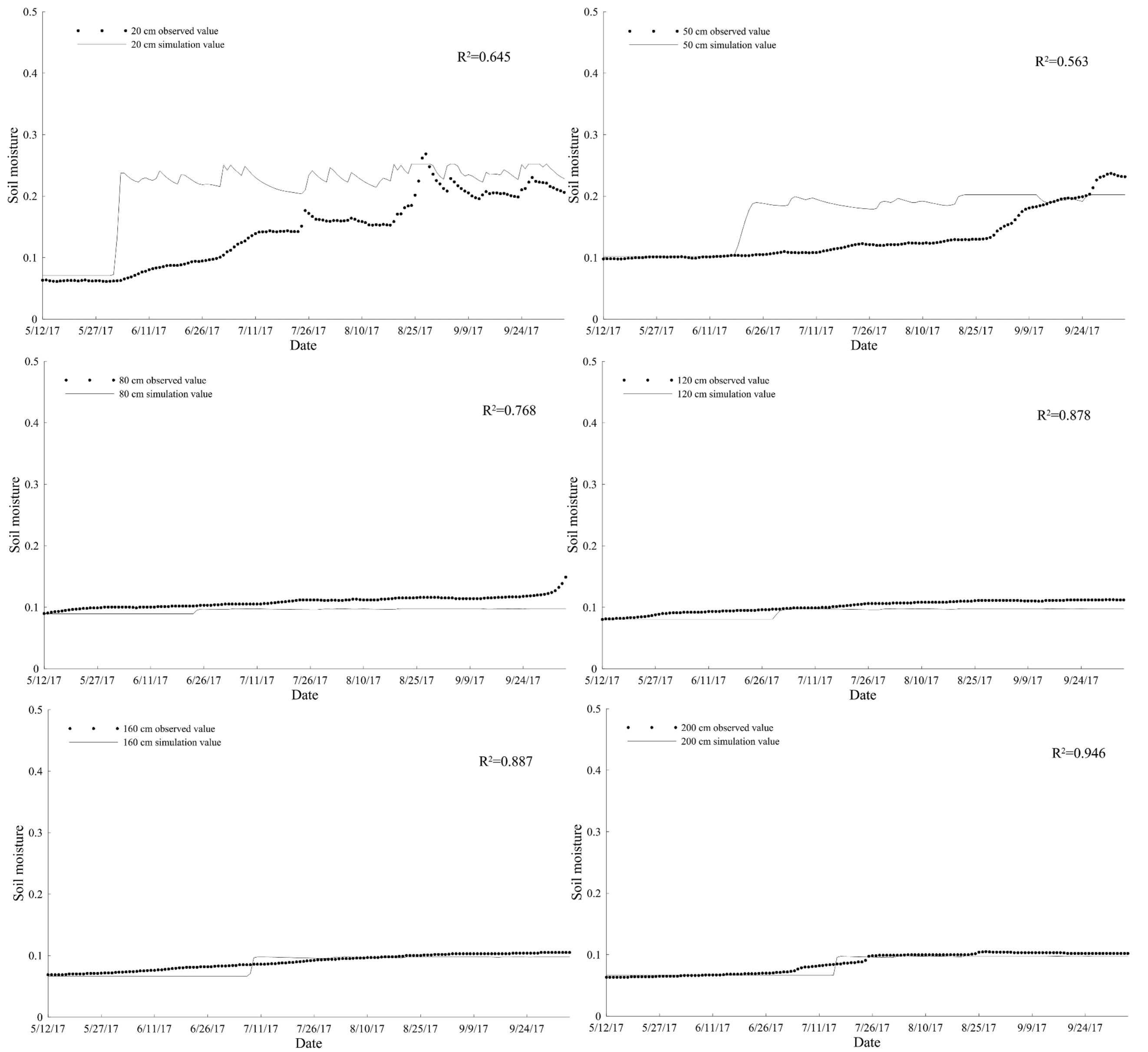

Figure 2d. Comparison of simulation results of soil temperature and moisture at different depths. (d) Soil moisture of seasonally frozen ground of the uphill slope.

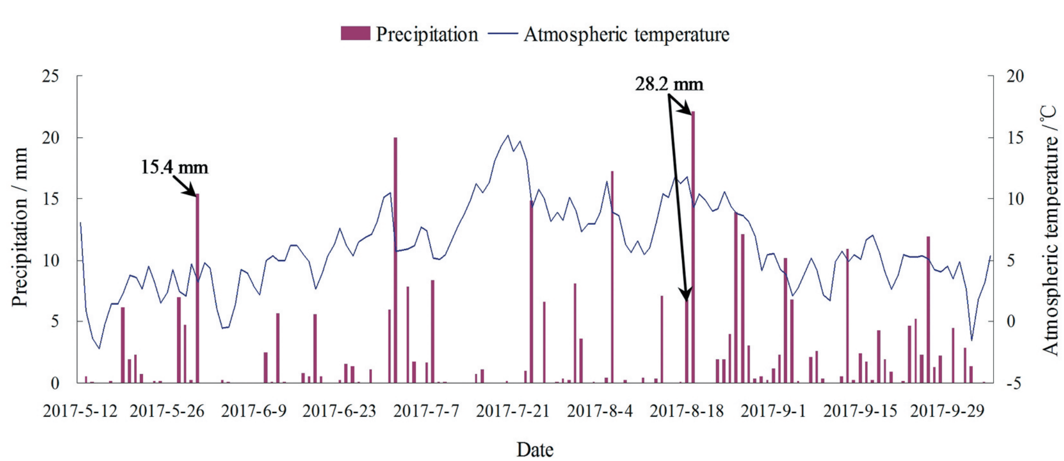

Figure 3. Temperature and precipitation of the study area.

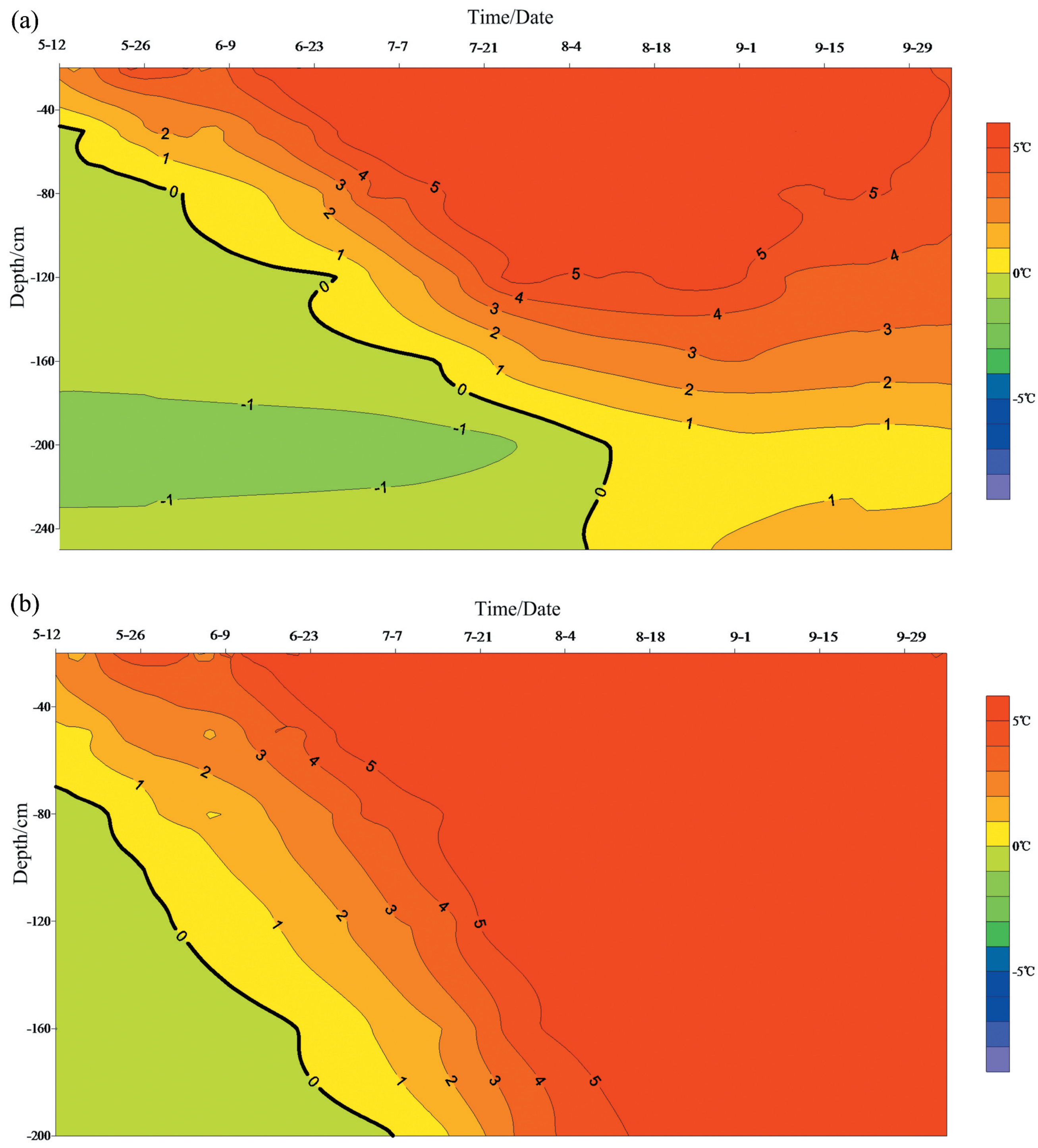

Figure 4. Contour lines of the soil temperature of (a) permafrost of the downhill slope and (b) seasonally frozen ground of the uphill slope.

surface soil increasing gradually, while the water content change of the bottom soil was not significant.

Based on the observations, the soil at depths of 20 cm and 50 cm had completely thawed by the beginning of May. So the soil in these layers was saturated and the soil volumetric water content remained stable, at about 30% and 40%, respectively. During the period from the end of May to the beginning of June, because the soil temperature at a depth of 80 cm of soil layer crossed the zero-degree isotherm, the soil in this layer entered the completely thawed state. During this period, the soil volumetric water content also increased rapidly, from about 10%, and reached a stable state at about 20%. The soil at depths of 120, 160, 200, and 250 cm entered a completely thawed state in late June, in early July, in the middle of July, and in early–mid August, respectively. At this time, the moisture content of each soil layer increased rapidly from 6% to 12%, from 6% to 37%, from 10% to 25%, and from 13% to 30%, respectively. During this period, although the frozen soil gradually thawed from the surface layer to the deep layer, the bottom soil was still in a frozen state. This means that rainfall

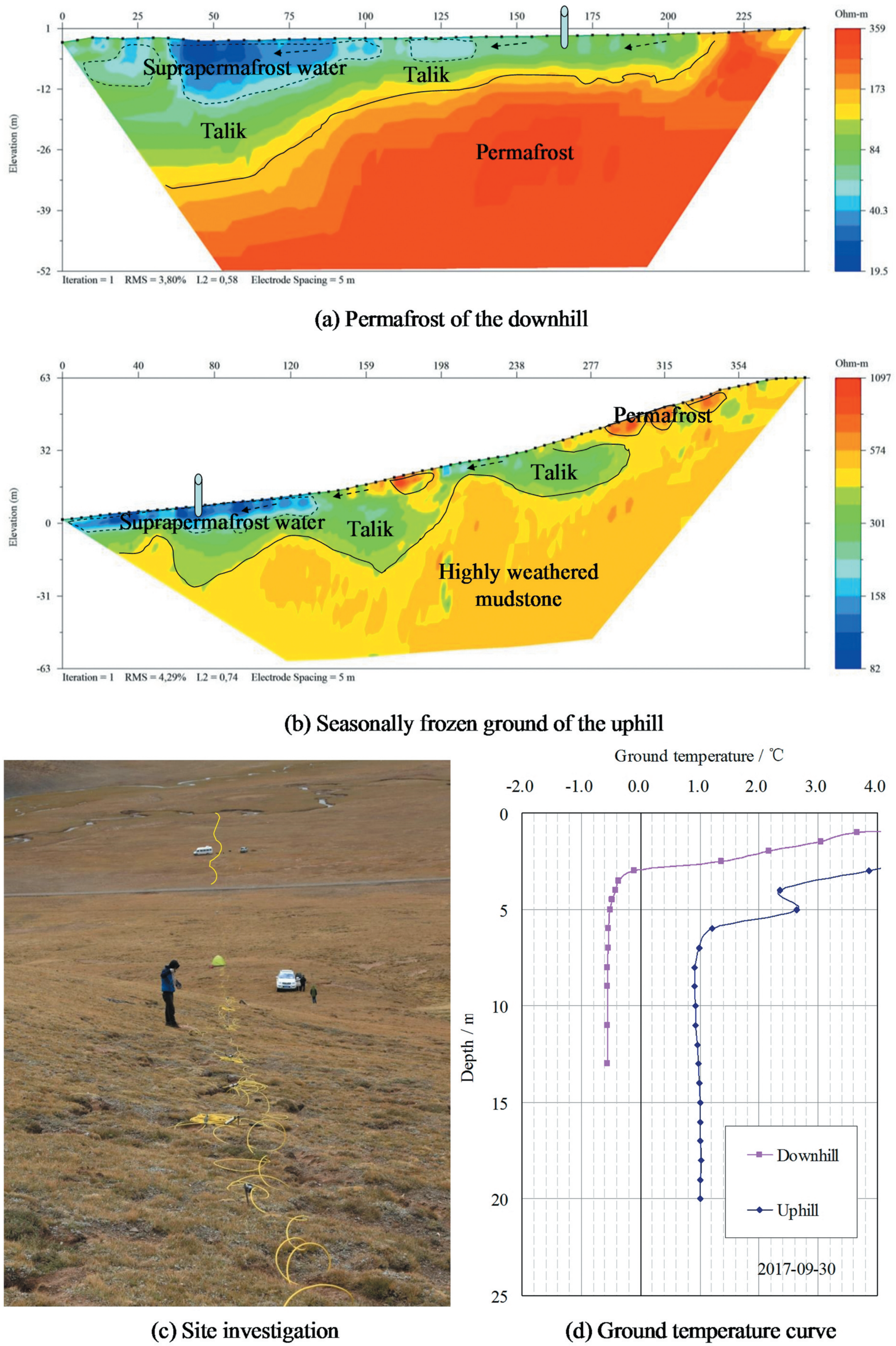

Figure 5. High-density electrical (ERT) inversion results of (a) permafrost of the downhill slope and (b) seasonally frozen ground of the uphill slope. (c) Photo of the site investigation. (d) Ground temperature curve.

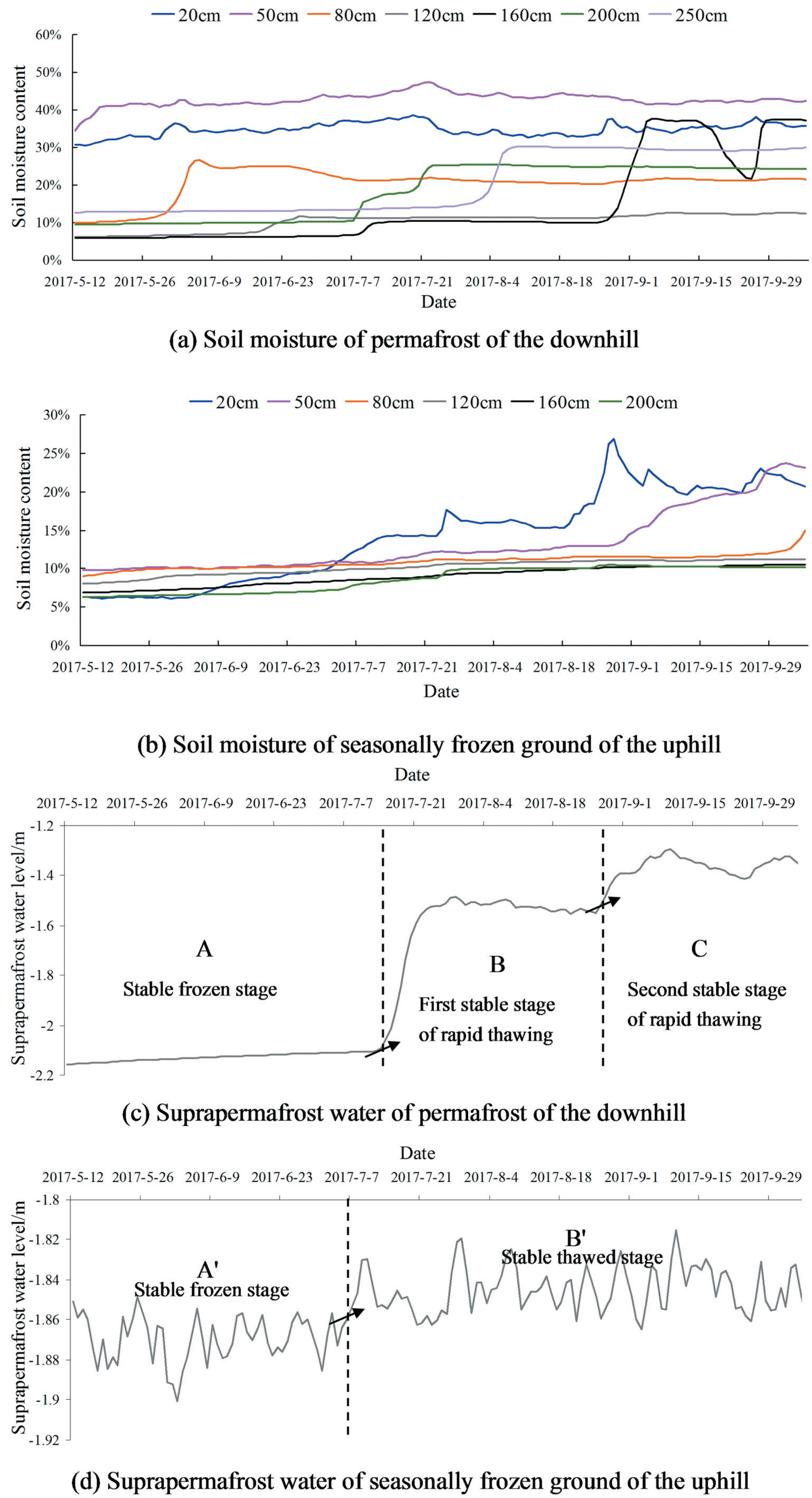

Figure 6. Seasonal change of soil hydrological process of soil moisture: (a) permafrost of the downhill slope and (b) seasonally frozen ground of the uphill slope. Suprapermafrost water of (c) permafrost of the downhill slope and (c) seasonally frozen ground of the uphill slope.

infiltration could not reach the bottom. Therefore, the observation of the suprapermafrost water shows that its variation is small, and it remains essentially unchanged.

The soil completely thawed by early–mid August. With the increase in rainfall, the water-storage capacity of the soil continued to increase gradually during the completely thawed stage. This led to the water-storage capacity of the soil reaching saturation. In particular, the soil water content of each layer is essentially saturated after late August, and its range of variation is not large. Because of the barrier effect of the lower permafrost layer, the observation of the suprapermafrost water level shows little change during this period. This indicates that the redistribution process of rainfall in permafrost regions is affected by the seasonal freeze–thaw process and the barrier of the permafrost layer. So the rainfall mainly infiltrates downward during the thawed period. This leads to a gradual increase in the soil water content of each layer. The soil water essentially achieves saturation when the soil completely thaws.

3.3.2 Seasonally frozen ground

Although the surface soil (0–50 cm) was completely thawed by early May, the volume of water content of the soil increased gradually in the seasonally frozen ground area of the uphill slope (Fig. 6). Because the surface soil thawed before the bottom soil, the lower soil (80–200 cm) remained completely frozen. This caused soil infiltration to fail to reach the bottom. With the thawing of soil from the surface layer to the deep layer, the lower soil moisture in each layer gradually increases to reach saturation during the rapid-thaw phase. However, because seasonally frozen ground experiences a short-term freeze–thaw process, the change of soil moisture is not obvious. In addition, because there is no permafrost layer acting as a barrier in the lower part, a stable aquiclude cannot be formed. Soil water at 200 cm seeps farther downward, resulting in an insufficient supply of soil water at this depth. Therefore, the surface soil water content increased gradually, while the lower soil water content changed little. The observation of the suprapermafrost water level during this period shows that its range of variation is small, and it remains essentially unchanged.

The soil layers were in a completely thawed state until 7 July. With the increase in rainfall, the soil water-storage capacity continued to increase gradually. It was not until September that the soil in each layer reached saturation. At the same time, the observation of the suprapermafrost water level during this period showed that its variation was small, and it remained essentially unchanged. This indicates that the redistribution of rainfall in seasonally frozen soil may be affected by other factors. Deep infiltration may not be the main form of rainfall infiltration.

3.4 Process of soil moisture infiltration in permafrost and seasonally frozen ground under typical rainfall events

We selected typical rainfall events during the rapid thaw period and the stable thaw period. Based on the monitoring data of field rainfall, we attempted to analyse the differences in the soil moisture infiltration process between permafrost area and seasonally frozen ground area. Figure 7 shows the changes in response to two typical rainfall events, one moderate and one heavy, in the soil moisture of permafrost and seasonally frozen ground.

A typical precipitation event in the rapid thaw period began at 00:00 and ended at 10:00 on 31 May 2017. It lasted 11 h and the accumulated rainfall was 15.4 mm (moderate rainfall). There was little other rain from the end of this rainfall episode until 10 June. A typical precipitation event during the stable thawed period began at 22:00 on 18 August 2017 and ended at 09:00 on 19 August 2017. It lasted 12 h and the accumulated rainfall was 28.2 mm (heavy rainfall). There was very seldom other rainfall after the end of the rainfall event.

The two typical precipitation events were as follows:

(1) **31 May 2017: Rapid thaw phase**. This period is in the thawed stage at 80 cm soil depth in the permafrost area of the downhill slope. By the end of this rainfall event, the surface soil (0–80 cm) was completely thawed and had reached saturation. So the water content of soil volume at 20 cm and 50 cm depths remained essentially unchanged. The water content of soil volume at 80 cm depth gradually increased under the effect of rainfall infiltration. But soil moisture content at this depth has a certain lag to the response of rainfall. This is mainly due to it taking time for soil moisture to penetrate from top to bottom. The figure shows that in the 24 h after the end of the rainfall event, soil moisture remained essentially unchanged. From 24 h to 130 h, soil moisture began to rise rapidly from about 12% to about 26%, and it reached a stable state after 130 h. The water content of the subsoil (80–250 cm) remained essentially unchanged due to being affected by the soil freezing.

(2) **19 August 2017: Stable thawed phase**. During this period, the frozen soil completely thawed in the permafrost area of the downhill slope and the seasonally frozen ground area of the uphill slope due to the higher atmospheric temperature. As can be seen from Fig. 7, by the end of this rainfall event, all layers of soil in the permafrost regions of the downhill had reached saturation. Therefore, soil volumetric water content at different depths remained essentially unchanged. Under the influence of rainfall infiltration, in addition to evaporation, soil moisture mainly infiltrated downward by vertical gravity gradient, which is an important recharge source of suprapermafrost water.

Moreover, the response of soil water content at 20 cm depth to rainfall also lagged. Within 240 h after the end of the rainfall event during the rapid thaw phase, the volumetric water content at 20 cm depth of topsoil increased from 6% to 8%, and it continued to increase gradually. Within 130 h after the end of the rainfall during the stable thawed phase, the volumetric water content of the 20 cm topsoil increased from 15% to only 18%. But 130 h after the end of the rainfall event, the volume water content of the soil increased rapidly. It reached the maximum value of about 27% within 190 h after the end of the rainfall. By this

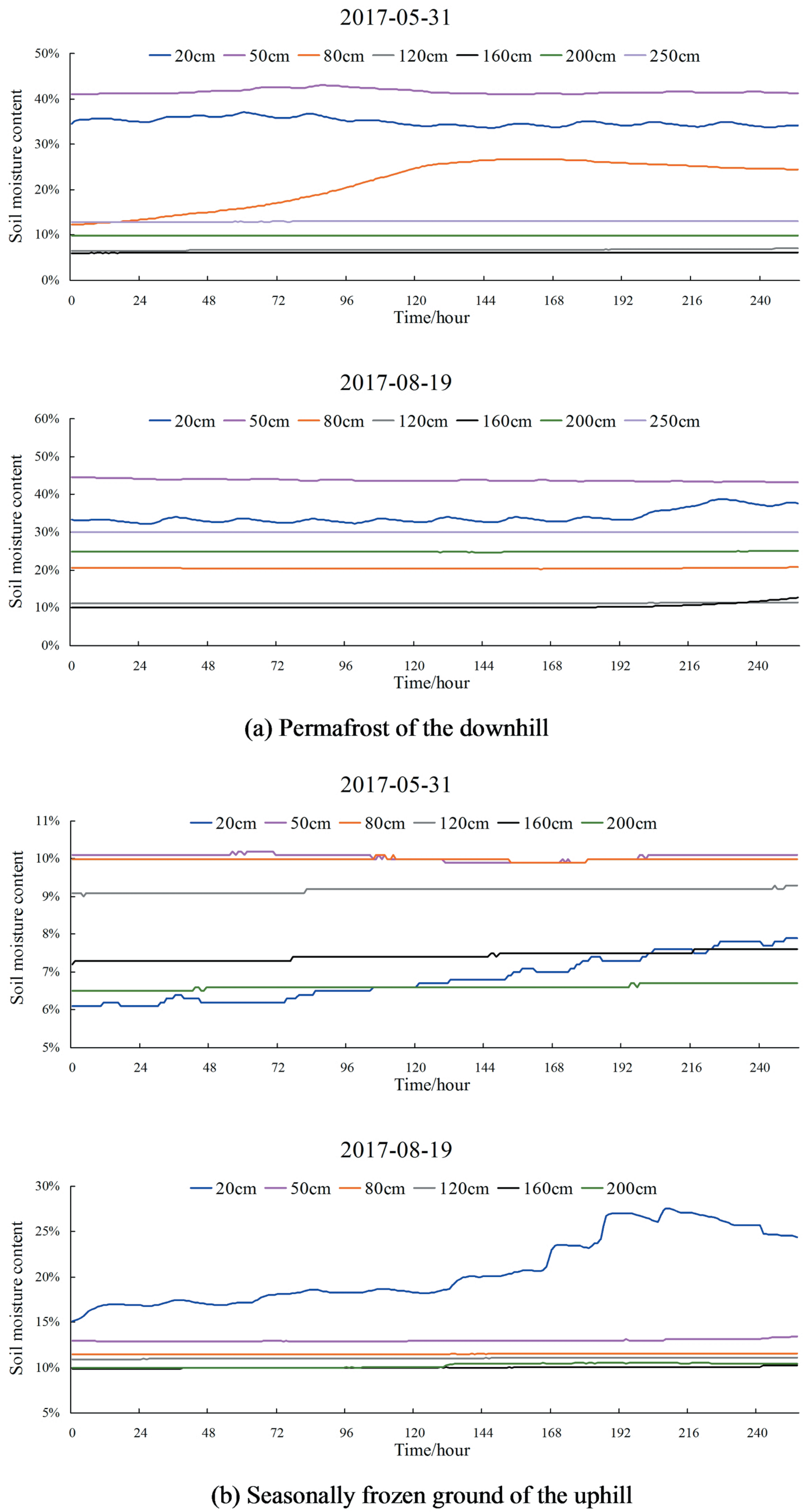

Figure 7. Response changes of typical rainfall events of the soil moisture of (a) permafrost of the downhill slope and (b) seasonally frozen ground of the uphill slope.

time, the soil was saturated. After that, the soil water content reached a stable state and remained essentially unchanged.

4 Discussion

4.1 Simulated changes in the soil moisture infiltration process in permafrost and seasonally frozen ground

We used the freeze–thaw module of the HYDRUS-1D software to simulate the soil water vertical infiltration of permafrost and seasonally frozen ground during the thawing period (May to October 2017). Figure 8 shows the variation in water storage and bottom leakage flux over time in permafrost and seasonally frozen ground.

We noted the following:

(1) In the rapid thaw phase, the water-storage capacity of the frozen soil began to increase gradually in the permafrost area of the downhill slope. This was mainly due to a large gravity gradient forming in the vertical direction of the soil, which led to the infiltration of soil moisture from top to bottom. As can be seen from Fig. 8, from early–mid May to mid–late August, soil water storage was rising and gradually reached its maximum value. During this period, because the frozen soil at the bottom had not completely thawed, the rainfall infiltration could not reach the bottom, and the flux at the bottom was relatively small. During the stable thawed stage, the soil water-storage capacity reached the saturated state. After mid–late August, rainfall became more frequent. This led to rainfall infiltrating from top to bottom. Because the soil water content of each layer reached the maximum saturated state, the soil water storage was essentially in a stable state. After vertical infiltration of rainfall into soil, bottom infiltration flux was generated in the form of interflow in soil. Because of the barrier effect of the permafrost layer, this

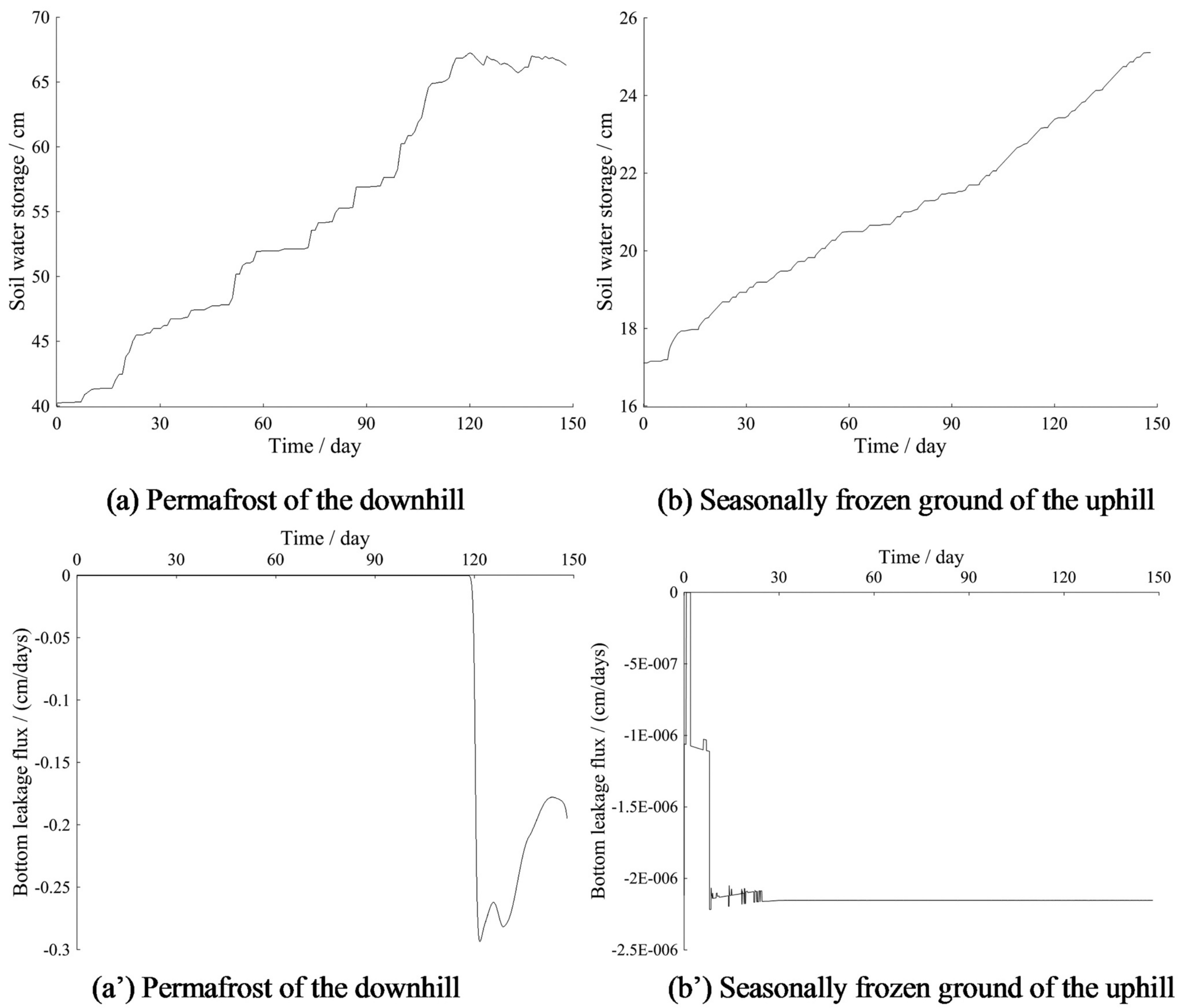

Figure 8. Simulated changes of soil water storage and bottom leakage flux of (a, a') permafrost of the downhill slope and (b, b') seasonally frozen ground of the uphill slope.

part of the water mainly recharges the suprapermafrost water, causing the rapid rise of the suprapermafrost water level and gradually reaching a stable state.

(2) The soil in the seasonally frozen ground area of the uphill slope had thawed completely by early–mid July. With the thawing of the frozen soil, the water storage capacity of the soil was gradually enhanced. Although the rainfall was gradually increasing during this period, without the barrier effect of the permafrost layer the infiltration capacity of each layer of soil was strong. This led to the difficulty of saturating the soil during this period. Therefore, the soil volumetric water content of each layer increased gradually. As can be seen from Fig. 6, the soil water storage of frozen soil in the seasonally frozen ground area of the uphill slope had been rising for some time, but it still did not reach a stable state. Although the frozen soil had completely thawed and the rainfall had increased during this period, rainfall infiltration did not discharge downward in the form of interflow. This meant that the soil water content in each layer on the upper slope was in the unsaturated state. So the bottom flux was relatively small.

Based on field monitoring and simulation analysis, we systematically summarize differences in the soil moisture infiltration process in permafrost and seasonally frozen ground in different thawing phases. The differences are shown in Table 1.

4.2 Factors influencing the soil moisture infiltration process in permafrost and seasonally frozen ground

Based on the above analysis, the main factor that distinguishes the soil moisture infiltration process in permafrost and seasonally frozen ground is freeze–thaw action. On the one hand, affected by freeze–thaw action, the soil thawing process of the active layer in the permafrost area will take a longer time (Fig. 4). As a result, the process of infiltration of soil moisture in the permafrost area is more susceptible to freeze–thaw action than that in the seasonally frozen ground area.

Figure 6 shows a significant increase in the moisture content of each soil layer from top to bottom in the permafrost area of the downhill slope. The topsoil water storage has been rising over time and cannot reach a stable state in the seasonally frozen ground area of the uphill slope, whereas the changes in moisture content of the other soil layers are not significant. On the other hand, Fig. 6 also shows that the response time of soil moisture infiltration to rainfall in the permafrost area lags behind that in the seasonally frozen ground area.

Moreover, local factors are also important factors influencing the soil moisture infiltration process in the seasonally frozen ground area. In particular, it may be more easily affected by factors such as soil texture, evaporation, terrain and infiltration capacity. On the one hand, the higher the soil organic matter content, the lower the soil heat conduction and the higher the soil thermal capacity. This reduces the sensitivity of the underlying soil thermal state to solar radiation and temperature fluctuations (Hinkel *et al*. 2001, Wang *et al*. 2014). At the same time, this will help to maintain the stability of soil moisture.

The topsoil organic matter content reaches 11.8 g/kg in the seasonally frozen ground area of the uphill slope, while it reaches 27.9 g/kg in the permafrost area of the downhill slope. This means that the soil moisture variability in the seasonally frozen ground area of the uphill slope is more affected by soil temperature than that in the permafrost area of the downhill slope. On the other hand, low vegetation coverage also leads to a strengthening of the evaporation capacity in the seasonally frozen ground area of the uphill slope (Hu *et al*. 2009, Wang *et al*. 2009). In addition, slope position affects the lateral loss of soil moisture. The greater the slope, the smaller the storage of soil moisture (Cao *et al*. 2017).

4.3 Does the groundwater in talik affect the change in the suprapermafrost water?

Figure 6 shows that the soil moisture contents at depths of 160 cm and 200 cm in the permafrost area of the downhill slope both increased rapidly in early–mid July. During this period, the soil at 160 cm had completely thawed, but the soil at 200 cm had not. Meanwhile, during this period, the suprapermafrost water in the permafrost area of the downhill slope changed from the stable frozen stage A to the rapid thaw stage B, and the water volume increased rapidly. Because the soil at the bottom was still frozen, the infiltration of rainfall at the top could not change the suprapermafrost water level, and because Kangqiong small basin is close to the river, the thermal erosion of the river makes the permafrost around it degenerate continuously. This leads to the deepening of the permafrost table and the expanding of the talik. Due to the influence of river water penetrating the talik, the hydraulic connection between the groundwater of the talik and the suprapermafrost is increased (Rowland *et al.* 2011, Wellman *et al.* 2013, Scheidegger and Bense 2014, Johansson *et al.* 2015, Kurylyk *et al.* 2016).

During early–mid July, the surface soil in the permafrost area of the downhill slope completely thaws, meaning that the groundwater in the talik channel may be saturated. A hydraulic connection occurs between the groundwater in the talik channel and the suprapermafrost water in the permafrost area of the downhill. As a result, soil water content at 200 cm depth in the downhill slope increases rapidly and gradually reaches a state of saturation. The groundwater in the talik channel may be the main source of water supplying the suprapermafrost water in the permafrost area of the downhill slope. This will

Table 1. Differences in the soil moisture infiltration process in permafrost and seasonally frozen ground in different thawing phases.

Types of frozen soil	Thawing phases	Rainfall infiltration	Soil moisture	Suprapermafrost water
Permafrost	Rapid thawing	Limitedly increasing	Gradually increasing	Slightly rising
	Stable thawing	Gradually increasing	Saturated state	Greatly rising
Seasonally frozen ground	Rapid thawing	Limitedly increasing	Gradually increasing	Slightly rising
	Stable thawing	Gradually increasing	Continuously increasing	Slightly rising

cause a rapid rise of the suprapermafrost water level in permafrost area of the downhill.

Figure 9 shows the seasonal variation of the suprapermafrost water temperature of the permafrost and the seasonally frozen ground areas in Kangqiong small basin. The water temperature of the suprapermafrost water in the permafrost area of the downhill slope changed from negative (−) to positive (+) only in mid–late July. This indicates that soil temperature, soil moisture, suprapermafrost water temperature and suprapermafrost water are still in the stage of transition from freeze to thaw in mid–late July. Rainfall infiltration is not enough to cause the rapid rise of soil moisture and suprapermafrost water level during this period. Therefore, this further confirms the presence of groundwater in the talik channel and a hydraulic connection between the groundwater in the talik channel and the suprapermafrost water in the permafrost area of the downhill slope.

By mid–late August, the soil at the bottom of the downhill slope has thawed completely and all soil layers are saturated. The

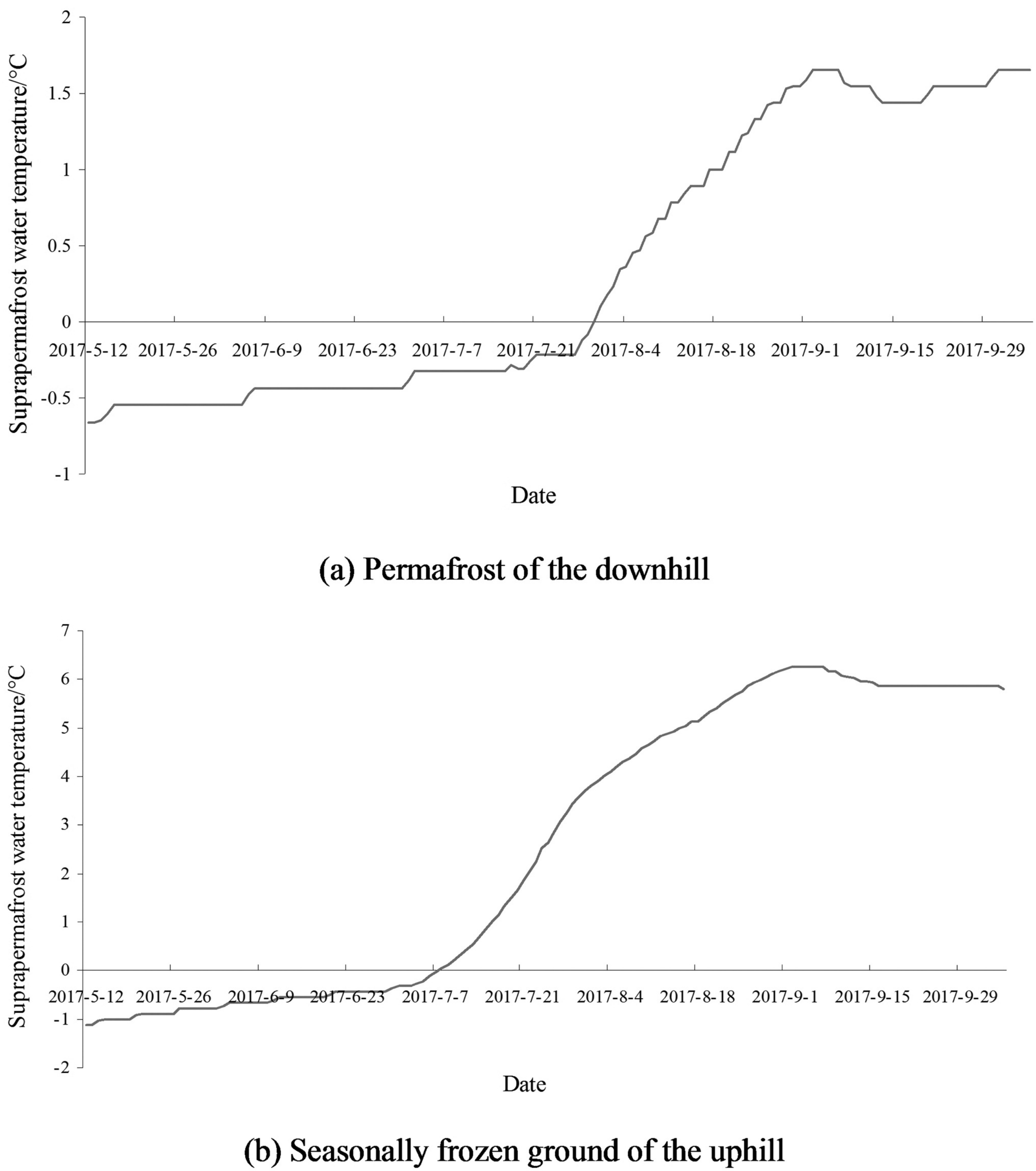

Figure 9. Seasonal change of the suprapermafrost water temperature of (a) permafrost and (b) seasonally frozen ground.

infiltration capacity of the soil is enhanced due to the increasing rainfall. Soil moisture will reach the bottom flowing from the top down. Because of the barrier effect of permafrost, soil moisture will accumulate at the bottom. This will lead to the secondary rise of the suprapermafrost water level. The first stable stage B of rapid thawing will be changed to the second stable stage C of rapid thawing.

The soil layers in the seasonally frozen ground area of the uphill slope have completely thawed by 7 July. During this period, the suprapermafrost water level of the uphill changes from the stable frozen stage of A' to the stable thawed stage of B', and the water volume has an increasing trend (Fig. 6). As the water-holding capacity of the lower soil (80–200 cm) is weak, the soil water content has not yet reached saturation in terms of its changing trend. Therefore, the soil infiltration driven by the upper rainfall is not enough to cause the change in the suprapermafrost water level of the uphill slope.

This is similar to the time of the first change of the suprapermafrost water level of the downhill slope and shows that there is a certain degree of hydraulic connection between the groundwater in the talik channel and the suprapermafrost water. The groundwater in the talik channel is saturated in mid–early July, leading to the suprapermafrost water level of the uphill rising to a certain extent. The nearer the river, the greater the recharge of groundwater in the talik channel to the suprapermafrost water. As a result, its main recharge affects the suprapermafrost water of the downhill and causes the rapid rise of the suprapermafrost water of the downhill.

Figure 8 shows the seasonal variation of the suprapermafrost water temperature of seasonally frozen ground in Kangqiong small basin. As can be seen from the figure, the water temperature of the suprapermafrost water in the seasonally frozen ground area of the uphill changed from negative (−) to positive (+) on 7 July. This shows that soil temperature, soil moisture, suprapermafrost water temperature and suprapermafrost water were all in the thawed stage on 7 July. The groundwater in the talik channel was in the saturated state and it recharged the suprapermafrost water in the seasonally frozen ground area of the uphill slope.

5 Conclusions

(1) During the rapid thaw phase, influenced by the freezing of the underlying soil, soil infiltration is limited. It leads only to a slight rise in the suprapermafrost water level. During the stable thawed stage, rainfall infiltration increases gradually, which leads to an increase in soil moisture content and an increase in soil water infiltration. In the permafrost area, due to the barrier effect of the permafrost layer, the interflow in the soil accumulates near the permafrost table. This leads to the suprapermafrost water level rising significantly. In the seasonally frozen ground area, soil water movement is dominated by lateral flow and downward infiltration.

(2) Influenced by freeze–thaw action, the infiltration process of soil moisture in the permafrost area is more stable than that in the seasonally frozen ground area. The response time of soil moisture infiltration to rainfall in the permafrost area also lags behind that in the seasonally frozen ground area. With the thawing of soil from the surface layer to the deep layer, the soil water content in the permafrost area gradually increases until it reaches a state of saturation. Rainfall loss is affected by terrain, soil texture, evapotranspiration and infiltration capacity, producing a large variation in the topsoil moisture content of the seasonally frozen ground area of the uphill slope.

(3) Groundwater in the talik is well developed in the Kangqiong small basin. By early–mid July, the soil has completely thawed. During this period, the groundwater in the talik is saturated. This leads to a slight increase in the suprapermafrost water level in seasonally frozen ground area of the uphill. In addition to rainfall infiltration, the change of the suprapermafrost water level in permafrost area of the downhill is also affected by groundwater in the talik. It mainly recharges the suprapermafrost water, which causes the rapid rise of the suprapermafrost water on the downhill slope.

Although many analyses have been carried out on the soil hydrological processes in permafrost areas and in seasonally frozen ground areas, this study is limited to the period of the field observation; in particular, the time series of monitored data of rainfall, soil moisture and suprapermafrost water level is relatively short. Thus, to some extent, this has restricted the study's potential to reveal the differences in soil water movement between the permafrost area and the seasonally frozen ground area. In addition, the hydraulic connection and relationship between the groundwater in the talik and the suprapermafrost water is only a small part of the hydrological processes affecting the permafrost area. All of the above requires more field-monitoring data in the future to verify the validity of the conclusions.

Acknowledgements

The authors thank the editors and anonymous reviewers for their insightful comments and suggestions that helped improve this paper. Useful suggestions given by Dr Gagarin Leonid from Melnikow Permafrost Institute, Siberian Branch Russian Academy of Sciences, are also acknowledged.

Disclosure statement

No potential conflict of interest was reported by the authors.

Funding

This work was supported by the National Natural Science Foundation of China [No. 41971093].

References

Bibi, S., *et al.*, 2018. Climatic and associated cryospheric, biospheric, and hydrological changes on the Tibetan Plateau: a review. *International Journal of Climatology*, 38 (1), E1–E17. doi:10.1002/joc.5411

Cao, W., *et al.*, 2017. Spatial variability and its main controlling factors of the permafrost soil-moisture on the northern-slope of Bayan Har Mountains in Qinghai-Tibet Plateau. *Journal of Mountain Science*, 14 (12), 2406–2419. doi:10.1007/s11629-017-4467-z

Chang, J., *et al.*, 2015. Seasonal dynamics of suprapermafrost groundwater and its response to the freeing-thawing processes of soil in the permafrost region of Qinghai-Tibet Plateau. *Science China Earth Sciences*, 58 (5), 727–738. doi:10.1007/s11430-014-5009-y

Chang, J., Ye, R.Z., and Wang, G.X., 2018. Review: progress in permafrost hydrogeology in China. *Hydrogeology Journal*, 26 (5), 1387–1399. doi:10.1007/s10040-018-1802-6

Cheng, G.D. and Jin, H.J., 2013. Permafrost and groundwater on the Qinghai-Tibet Plateau and in northeast China. *Hydrogeology Journal*, 21 (1), 5–23. doi:10.1007/s10040-012-0927-2

Dagois, R., *et al.*, 2017. From atmospheric- to pedo-climate modeling in Technosols: a global scale approach. *Geoderma*, 301, 47–59. doi:10.1016/j.geoderma.2017.04.011

Guan, X.J., Spence, C., and Westbrook, C.J., 2010b. Shallow soil moisture-ground thaw interactions and controls-Part 2: influences of water and energy fluxes. *Hydrology and Earth System Sciences*, 14 (7), 1387–1400. doi:10.5194/hess-14-1387-2010

Guan, X.J., Westbrook, C.J., and Spence, C., 2010a. Shallow soil moisture-ground thaw interactions and controls-Part 1: spatiotemporal patterns and correlations over a subarctic landscape. *Hydrology and Earth System Sciences*, 14 (7), 1375–1386. doi:10.5194/hess-14-1375-2010

Hansson, K., *et al.*, 2004. Water flow and heat transport in frozen soil: numerical solution and freeze/thaw applications. *Vadose Zone Journal*, 3 (2), 693–704. doi:10.2136/vzj2004.0693

Hinkel, K.M., *et al.*, 2001. Patterns of soil temperature and moisture in the active layer and upper permafrost at Barrow, Alaska: 1993-1999. *Global and Planetary Change*, 29 (3–4), 293–309. doi:10.1016/S0921-8181(01)00096-0

Hu, H.C., *et al.*, 2009. Response of soil heat-water processes to vegetation cover on the typical permafrost and seasonally frozen soil in the headwaters of the Yangtze and Yellow Rivers. *Chinese Science Bulletin*, 54 (2), 242–250.

Jafarov, E.E., *et al.*, 2018. Modeling the role of preferential snow accumulation in through talik development and hillslope groundwater flow in a transitional permafrost landscape. *Environmental Research Letters*, 13 (10), 105006. doi:10.1088/1748-9326/aadd30

Jepsen, S.M., *et al.*, 2013. Sensitivity analysis of lake mass balance in discontinuous permafrost: the example of disappearing Twelvemile Lake, Yukon Flats, Alaska (USA). *Hydrogeology Journal*, 21 (1), 185–200. doi:10.1007/s10040-012-0896-5

Jin, H.J., *et al.*, 2006. Thermal regimes and degradation modes of permafrost along the Qinghai-Tibet highway. *Science in China Series D-Earth Sciences*, 49 (11), 1170–1183. doi:10.1007/s11430-006-2003-z

Johansson, E., *et al.*, 2015. Data evaluation and numerical modeling of hydrological interactions between active layer, lake and talik in a permafrost catchment, Western Greenland. *Journal of Hydrology*, 527, 688–703. doi:10.1016/j.jhydrol.2015.05.026

Jones, B.M., *et al.*, 2016. Presence of rapidly degrading permafrost plateaus in south-central Alaska. *Cryosphere*, 10 (6), 2673–2692. doi:10.5194/tc-10-2673-2016

Jorgenson, M.T., *et al.*, 2010. Resilience and vulnerability of permafrost to climate change. *Canadian Journal of Forest Research-Revue Canadienne De Recherche Forestiere*, 40 (7), 1219–1236. doi:10.1139/X10-060

Kurylyk, B.L., *et al.*, 2016. Influence of vertical and lateral heat transfer on permafrost thaw, peatland landscape transition, and groundwater flow. *Water Resources Research*, 52 (2), 1286–1305. doi:10.1002/2015WR018057

Lamontagne-Halle, P., *et al.*, 2018. Changing groundwater discharge dynamics in permafrost regions. *Environmental Research Letters*, 13 (8), 084017. doi:10.1088/1748-9326/aad404

Li, R.P., *et al.*, 2012. Simulation of freezing and thawing soils in Inner Mongolia Hetao Irrigation District, China. *Geoderma*, 173, 28–33.

Oliva, M., Pereira, P., and Antoniades, D., 2018. The environmental consequences of permafrost degradation in a changing climate. *Science of the Total Environment*, 616, 435–437. doi:10.1016/j.scitotenv.2017.10.285

Rowland, J.C., Travis, B.J., and Wilson, C.J., 2011. The role of advective heat transport in talik development beneath lakes and ponds in discontinuous permafrost. *Geophysical Research Letters*, 38, L17504. doi:10.1029/2011GL048497

Scheidegger, J.M. and Bense, V.F., 2014. Impacts of glacially recharged groundwater flow systems on talik evolution. *Journal of Geophysical Research-Earth Surface*, 119 (4), 758–778. doi:10.1002/2013JF002894

Schuh, C., Frampton, A., and Christiansen, H.H., 2017. Soil moisture redistribution and its effect on inter-annual active layer temperature and thickness variations in a dry loess terrace in Adventdalen, Svalbard. *The Cryosphere*, 11 (1), 635–651. doi:10.5194/tc-11-635-2017

Subin, Z.M., *et al.*, 2013. Effects of soil moisture on the responses of soil temperatures to climate change in cold regions. *Journal of Climate*, 26 (10), 3139–3158. doi:10.1175/JCLI-D-12-00305.1

Wang, G.X., *et al.*, 2009. Water regime shifts in the active soil layer of the Qinghai-Tibet Plateau permafrost region, under different levels of vegetation. *Geoderma*, 149 (3–4), 280–289. doi:10.1016/j.geoderma.2008.12.008

Wang, G.X., *et al.*, 2014. Impacts of surface soil organic content on the soil thermal dynamics of alpine meadows in permafrost regions: data from field observations. *Geoderma*, 232, 414–425. doi:10.1016/j.geoderma.2014.05.016

Wang, X.Q., Chen, R.S., and Yang, Y., 2017. Effects of permafrost degradation on the hydrological regime in the source regions of the Yangtze and Yellow Rivers, China. *Water*, 9 (11), 897. doi:10.3390/w9110897

Wellman, T.P., Voss, C.I., and Walvoord, M.A., 2013. Impacts of climate, lake size, and supra- and sub-permafrost groundwater flow on lake-talik evolution, Yukon Flats, Alaska (USA). *Hydrogeology Journal*, 21 (1), 281–298. doi:10.1007/s10040-012-0941-4

Woo, M.K., *et al.*, 2008. Progress in permafrost hydrology in the New Millennium. *Permafrost and Periglacial Processes*, 19 (2), 237–254. doi:10.1002/ppp.613

Wu, J.C., *et al.*, 2010. Processes and modes of permafrost degradation on the Qinghai-Tibet Plateau. *Science China: Earth Sciences*, 53 (1), 150–158. doi:10.1007/s11430-009-0198-5

Wu, Q.B. and Zhang, T.J., 2008. Recent permafrost warming on the Qinghai-Tibetan plateau. *Journal of Geophysical Research-Atmospheres*, 113 (D13), D13108. doi:10.1029/2007JD009539

Yang, Z.P., *et al.*, 2011. Spatial variability of soil moisture at typical alpine meadow and steppe sites in the Qinghai-Tibetan Plateau permafrost region. *Environmental Earth Sciences*, 63 (3), 477–488. doi:10.1007/s12665-010-0716-y

You, Y.H., *et al.*, 2017. Thermal effects of lateral supra-permafrost water flow around a thermokarst lake on the Qinghai-Tibet Plateau. *Hydrological Processes*, 31 (13), 2429–2437. doi:10.1002/hyp.11193

Zhang, T.J., 2012. Progress of global permafrost and climate change studies. *Quarternary Sciences*, 32 (1), 27–38. (In Chinese).

Zhang, Y.S., *et al.*, 2015. Hillslope patterns in thaw-freeze cycle and hydrothermal regimes on Tibetan Plateau. *Chinese Science Bulletin*, 60 (7), 664–673. (In Chinese). doi:10.1360/N972014-00313

Zhao, X.B., *et al.*, 2019. Moisture distribution in sloping black soil farmland during the freeze-thaw period in Northeastern China. *Water*, 11 (3), 536. doi:10.3390/w11030536

Zhao, Y., *et al.*, 2016. Modeling of coupled water and heat transfer in freezing and thawing soils, Inner Mongolia. *Water*, 8 (10), 424. doi:10.3390/w8100424